Proceedings of the 10th World Congress on Civil, Structural, and Environmental Engineering (CSEE 2025)
Barcelona, Spain - April, 2025
Paper No. ICSECT 142
DOI: 10.11159/icsect25.142

DSM For Web Crippling Strength of Flange Fastened Lipped CFS Channels under ITF Loading: A Comprehensive Investigation

Hari Krishnan K P[1], Anil Kumar M V[2]
[1]PhD Scholar, Department of Civil Engineering, Indian Institute of Technology Palakkad,
Palakkad, Kerala, 678623, India, E-Mail: 102004003@smail.iitpkd.ac.in
[2]Associate Professor, Department of Civil Engineering, Indian Institute of Technology Palakkad,
Palakkad, Kerala, 678623, India, E-Mail: anil@iitpkd.ac.in

Abstract - The Direct Strength Method (DSM) is used for the computation of the design strength of members whose behavior is governed by any form of buckling. DSM based semi-empirical equations have been successfully used for cold-formed steel (CFS) members subjected to compression, bending, and shear. The DSM equations for the a CFS member strength are based on the parameters accounting for strength [yield load (P_y), yield moment (M_y), and shear yield load (V_y) for compression, bending, and shear respectively] and stability [buckling load (P_{cr}), buckling moment (M_{cr}), and shear buckling load (V_{cr}) for compression, bending and shear respectively]. The buckling of column and beam shall be governed by local, distortional, or global buckling modes and their interaction. Recently DSM- based methods are extended for the web crippling strength of CFS beams also. Numerous DSM-based expressions were reported in the literature which is the function of loading case, cross-section shape, and boundary condition. Unlike members subjected to axial load, bending, or shear, no unified expression for the design web crippling strength irrespective of the loading case, cross-section shape, and end boundary conditions are available yet. This study based on nonlinear finite element analysis (FEA) results shows that slenderness of the web, which shall be represented either using web height to thickness ratio (*h/t*) or P_{cr} has negligible contribution to web crippling strength for flange fastened lipped channel beam sections under interior two flanged (ITF) loading. Hence, the results in this paper question the suitability of DSM approach for the for the CFS beams' web crippling strength.

Keywords**:** cold-formed steel beams, DSM, interior two flanged loading (ITF) and web crippling.

1. Introduction

Recently, thin-walled sections have been increasingly utilized in cold-formed steel (CFS) construction due to technological advancements that produce high-strength steels with favourable strength-to-weight ratios. They are commonly used as floor support structures, decks, purlins, and bearers within variety of buildings types, where these components are often subjected to concentrated, localized loads that may result in web crippling, also referred to as local bearing failure. While there are numerous possible cross-sections, lipped and unlipped channels (Fig. 1(a) and 1(b)) are two of the most frequently employed. These channels have webs that are not reinforced, making them vulnerable to web crippling failure. Research on web crippling has primarily been conducted in renowned universities globally since the 1940s.

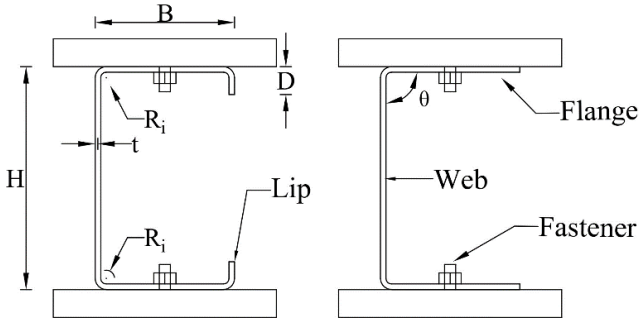

Fig. 1: Typical (a) lipped and (b) unlipped channel sections.

The complex nature of web crippling contributed to the experimental nature of these studies. The provisions presented in (EN-1993-1-3, 2005) and the unified crippling strength equation in (AISI S100, 2016) were derived, respectively, from the outcomes of these experimental investigations. While these experiments yield a substantial quantity of data regarding the web crippling capacity of CFS beams, most of them failed to validate the test procedure presented in (AISI S909, 2013). The precision of these equations was therefore dependent on cold-formed sections, geometric limits, loading conditions, and boundary conditions. Subsequently, as computational power progressed, numerical investigations employing nonlinear finite element (FE) models were widely employed to examine the crippling behavior from as early as 1989. This was accomplished with the utilization of diverse software packages such as ADINA [4], ANSYS [5], [6], [7] and ABAQUS [8], [9], [10], [11], [12]. After the FE models had been verified as accurate by comparison with test data, they were then utilized to conduct a parametric study.

The recent introduction of direct strength method (DSM) [13] into various design standards (AISI S100, 2016 and AS/NZS 4600, 2018) has led to a surge in studies aiming to expand DSM's capabilities to predict web crippling strength by idealizing it as a yielding - buckling interaction problem. DSM for ultimate strength uses two basic input values; yield load (P_y) and elastic buckling load (P_{cr}). Many DSM based expressions were proposed by various researchers which are mainly functions of the loading case, cross-section shape, and flange boundary conditions. The DSM based equations are expressed generally as given in Eqn. 1a to Eqn. 1d respectively. Regression analysis [14] was employed to propose the values of the coefficients *a*, *b*, *c*, *d*, and *e* based on the numerical results and test results.

$$\frac{P_u}{P_y} = 1 \qquad ; \lambda \leq d \tag{1a}$$

$$\frac{P_u}{P_y} = \left[1 + \left(1 - \frac{\lambda}{d}\right)(e-1)\right] \qquad ; \lambda \leq d \tag{1b}$$

$$\frac{P_u}{P_y} = 1.8 - 0.85\lambda^2 \qquad ; \lambda \leq d \tag{1c}$$

$$\frac{P_u}{P_y} = c\left[1 - a\left(\frac{1}{\lambda}\right)^{2b}\right]\left(\frac{1}{\lambda}\right)^{2b} \qquad ; \lambda > d \tag{1d}$$

Here, the parameter P_{cr} represents the elastic buckling load, which can be determined using either the available unified codal expression (AISI S100, 2016), or through a linear buckling analysis utilizing FEA software packages (e.g., ABAQUS [12]) or FSM software (e.g., THIN-WALL-2 V2.0 [15]). On the other hand, the parameter P_y corresponds to the yield load for web crippling, calculated based on yield line theory assuming various collapse mechanisms [11], [15]. This can be represented as a function involving the yield stress (f_y), web thickness (t), yield line length (N_m - a function of h, R_i, N, and t), and the inside bend radius measured along the section's middle ($R_m = R_i + t/2$). The general form for expressions of P_y are given in Eqn. 2a [12] and Eqn. 2b [15]. Here the values of k_1, k_2, k_3, k_4, a_1, a_2, and γ are all functions of the loading case and the member cross-section geometry. Although multiple expressions are provided in literature for calculating P_y and P_{cr}, no experimental validation of these expressions is reported yet.

$$P_y = k_1\left(\frac{N_m}{t}\right) \times \left(\sqrt{k_2\left(\frac{R_m}{t}\right)^2 + k_3} - k_4\left(\frac{R_m}{t}\right)\right) \times f_y t^2 \tag{2a}$$

$$P_y = \frac{(a_1 N_{m1} + a_2 N_{m2})}{4\gamma R_m} \times f_y t^2 \tag{2b}$$

In general, these DSM based expressions as in Eqn. 1a and Eqn. 1d are adopted by bulk of the literature [11], [14], [16], [17] which is essentially multiplying the bending strength term (P_y) with reduction or enhancement factor that is a function of non-dimensional slenderness ratio$\left(\lambda = \sqrt{P_y / P_{cr}}\right)$. There have also been recent studies considering the inelastic reserve capacity (when $P_u > P_y$) particularly for lower values on non-dimensional slenderness (λ). [15] proposed Eqn. 1b and Eqn. 1d with a mechanism strengthening effect coefficient (e). [12] proposed Eqn. 1c and Eqn. 1d for unfastened lipped channels subjected to ITF loading. The reasons for the availability of this inelastic reserve capacity were not explained in any of these studies. In this study, the DSM expressions and design procedure given in [15] were used for checking suitability of DSM based expressions for flange fastened lipped channels. This study mainly focuses on the use of the FEA results and show the minimal impact of web slenderness, which shall be represented either using web height to thickness ratio (h/t) or P_{cr} value for lipped channel beams (LCBs) subjected to ITF loading with flanges fastened to supports which in turn questions suitability of DSM based design approach for web crippling phenomenon.

2. FE Modelling and Validation

This section describes finite-element (FE) models that simulate web crippling and estimate the elastic buckling load (P_{cr}) of flange fastened LCBs subjected to ITF loading. The FE models consisting of three parts (one LCB member placed in between and fastened to two rigid bearing plates), were developed using ABAQUS/CAE 2020. A nonlinear general static analysis procedure was followed as reported in many recent studies [8], [9], [18], [19] to simulate the web crippling behavior of specimens and determine the web crippling strength ($P_{u\text{-}FEA}$) where as a linear perturbation procedure was utilized to perform the buckling analysis to determine the elastic buckling load, P_{cr} as explained in [11]. As a part of validation, five LCBs (with section thickness varies between 1.16 mm and 1.45 mm, while the web depth ranges from 121 mm to 300 mm respectively) under ITF loading case with varying bearing lengths (30 mm and 60 mm) as reported in [20] and confirming to the latest standard test method AISI S909 (2013) were selected. Table. 1 enlists the specimens' dimensions and material properties along with the comparison of experimental and simulation results. Various notation used in the table is as shown in Fig. 1. The centre-line dimensions obtained from the measured dimension were utilised to precisely simulate the LCB section in ABAQUS/ CAE 2020.

Table 1: Measured dimensions and material properties of specimens as reported in [20].

Specimen	H (mm)	t (mm)	R_i (mm)	L (mm)	f_y (mm)	$P_{u\text{-}exp}$ (kN)	P_{cr} (kN)	h/t	$\left(\frac{P_{u-exp}}{P_{u-FEA}}\right)$	$\left(\frac{P_{cr}}{P_{cr-FEA}}\right)$
C120-7-30-F	121	1.45	7	610	332	10.70	21.28	71.79	1.05	1.05
C120-10-30-F	121	1.45	10	610	332	9.96	23.44	67.66	1.04	1.08
C120-10-60-F	121	1.45	10	610	332	11.00	24.75	67.66	1.01	1.01
C200-7-60-F	200	1.16	7	1220	328	7.56	6.57	158.34	1.05	1.03
C300-7-60-F	300	1.45	7	1500	448	11.60	7.21	195.24	1.01	0.93

Numerical studies were conducted using a single LCB section as reported in (Sundararajah et al., 2017). The simulations use three-dimensional deformable shell elements (S4R) to model LCB sections, while four-noded rigid body elements (R3D4) were used to model the bearing plates, as depicted in Fig. 2. It also shows typical meshing scheme followed for the lipped channel section and the bearing plates (loading and support plates). The channel portion underwent a mesh size sensitivity investigation to see how element size affects accuracy and analysis time. Thus, finite element mesh sizes ranged from (3 × 3) mm^2 (length × width) to (5 × 5) mm^2 as reported by [7] depending on the LCB section dimensions. A finer mesh, consisting of nine elements, was employed to model the inside bent radius portions at the flange web corners. This was done because it has been documented that the meshing has a notable influence on the web crippling behaviour [21]. Furthermore, the mesh sensitivity analysis of rigid body elements to model the loading and support bearing plates showed

minimal impact on the results. Hence a coarser mesh size of 20 × 20 mm^2 was used. ABAQUS/CAE 2020 uses true stress and logarithmic plastic strain relationship were derived from the engineering stress versus strain data obtained from tensile coupon results in corresponding literature including strain-hardening effects.

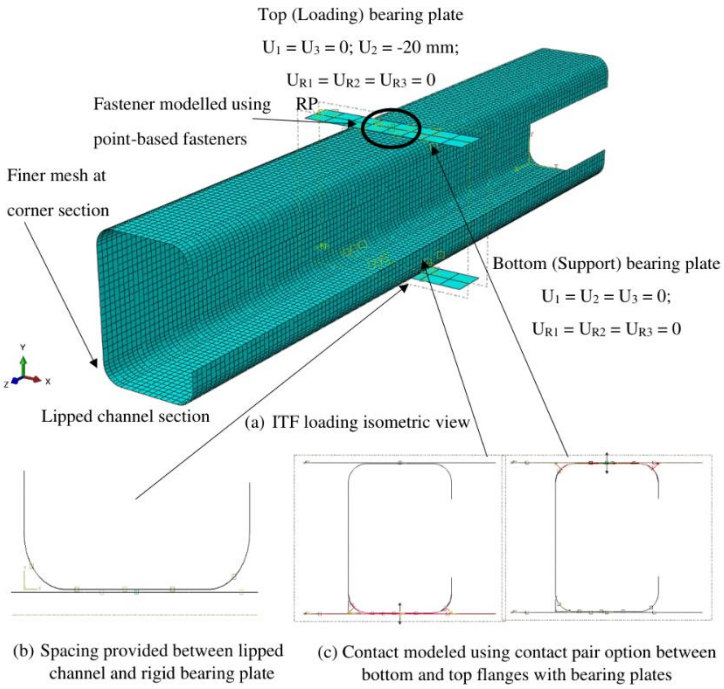

Fig 2: FE model developed for non-linear general static analysis of flange fastened LCB under ITF loading

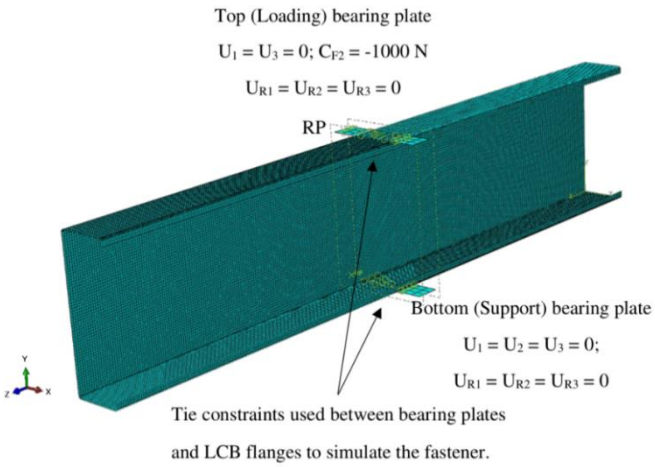

Fig 3: FE model developed for linear perturbation analysis of flange fastened LCBs under ITF loading

The bearing plates were subjected to appropriate boundary conditions at their respective reference points, indicated as RP in Fig. 2(a). The top bearing plate was subjected to vertical displacement, utilizing a smooth step amplitude to gradually apply loading on the LCB flange portion, with a maximum limit of either 12 mm or 20 mm, depending on whether the peak load was achieved. The translations along the other lateral directions, as well as the rotation about the vertical and horizontal axes of the loading plate, were prevented. Bottom bearing plate had similar boundary conditions to top ones, but vertical displacement was arrested.

The support bearing plate and the loading plate were positioned at a distance equal to half the thickness of the LCB section (t/2), as depicted in Fig. 2(b). This was done to ensure accurate representation of the LCB section in the shell FE model following the use of center-line dimensions. The separation between the flanges of LCBs and the plates was applied using face-to-face position constraints in ABAQUS. This was done for preventing any over-closure issues in-between the rigid surfaces of the rigid plates and the LCB flanges.

The simulation involved modelling the interactions between LCB flanges and bearing plates by utilizing surface-to-surface contact between the finite element model of the LCB shell and the rigid plates that represent the bearing plates to accurately simulate their actual behavior, as depicted in Fig. 2(c). Separation was allowed for surfaces that were in contact after the initial contact. While the tangential behavior was defined by using coefficient of friction value 0.4 between the surfaces [22], the normal behavior was defined using hard-contact with pressure over-closure and linear contact stiffness behavior using a value of 8000 calculated using the empirical equation as given in [10].

Initial geometric imperfection was also not considered while modeling, since it was reported to have negligible effect on the ultimate web crippling strength by [10] and [22] respectively.

The linear perturbation procedure type was used to perform buckling analysis to estimate the elastic critical buckling buckling load, P_{cr} of these specimens. The FE model developed for buckling analysis along with various boundary conditions conditions applied through respective reference points (denoted as RP) is shown in Fig. 3. The vertical displacement, U_2 was U_2 was kept free for top (loading) bearing plate and a concentrated load (C_{F2}) of magnitude 1000 N was applied at that reference point. The meshing scheme for both LCB and bearing plate sections are same as that used for non-linear static static analysis. However, the interaction between LCB flanges and bearing plates were not modeled using contact as it would lead to run time errors due to non-linearities arising from surface-to-surface contact. Thus, tie constraints were utilized to simulate the fasteners in these models as recommended in [10]. The accuracy of these developed models was then verified against the experiment results reported in [20] as a part of validation and reported in Table. 1.

The study compares the maximum web crippling strength obtained from numerical analyses and experimental research ($P_{u\text{-}FEA}$ and $P_{u\text{-}exp}$) for ITF loading by calculating the ratio ($P_{u\text{-}exp}/ P_{u\text{-}FEA}$). In addition, the table also compares the critical buckling loads obtained from literature with those calculated using ABAQUS/CAE 2020 (P_{cr} and $P_{cr\text{-}FEA}$) through linear buckling analysis, using the ($P_{cr} / P_{cr\text{-}FEA}$) ratio. The average ($\mu$) and coefficient of variation (*COV*) for web crippling strength ratios of LCB sections, as determined from tests and FEA, were 1.03 and 0.017, respectively. Similarly, the μ and *COV* of the buckling load were 1.02 and 0.049, respectively. The comparisons show the accuracy of the FE models developed in this study utilizing the nonlinear general-static analysis method to simulate the web crippling behaviour of fastened LCBs subjected to ITF loading.

3. Parametric study and DSM expression evaluation

The FE model developed in previous section is used for a detailed parametric study to investigate the effect of web-slenderness (using h/t or P_{cr}) on the ultimate load for flange fastened LCBs under ITF loading. Further the performance of DSM expression proposed by [15] is also investigated by comparing it with the simulation results using the ($P_{u\text{-}DSM} / P_{u\text{-}FEA}$) value. The parametric study involved the development of thirty-three models. Among these, eighteen models were having a section thickness of 1.2 mm, while the remaining fifteen models had a thickness of 2 mm. All specimens were having same inside radius, R_i = 4 mm, lip depth, D = 20 mm (except for 100 mm specimen with D = 15 mm), yield stress, f_y = 400 MPa, Young's Modulus, E = 203000 MPa and Poisson's ratio value, ν = 0.3 respectively.

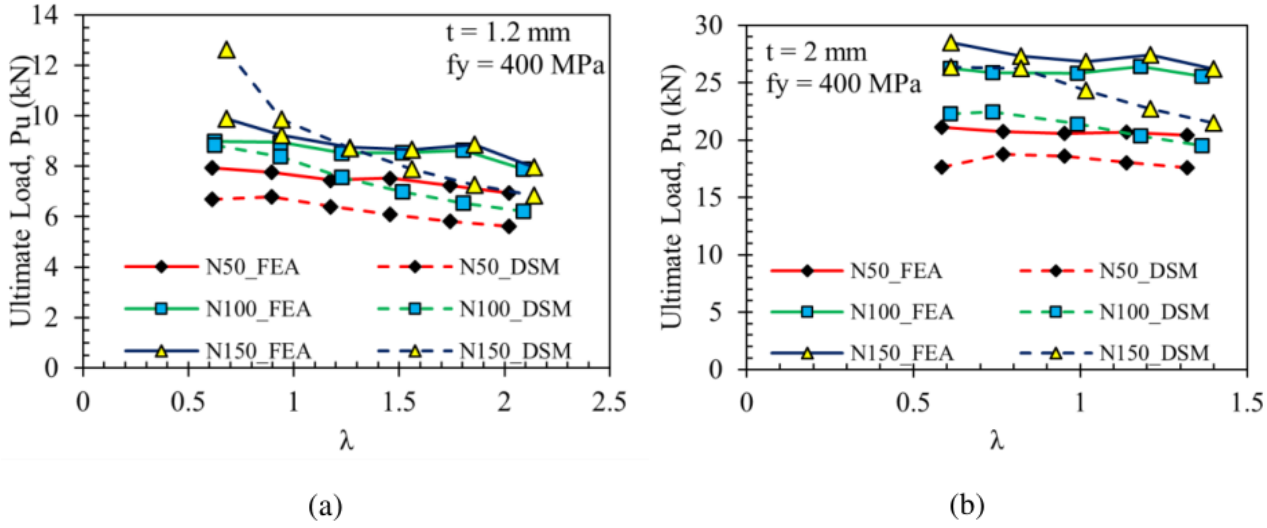

Fig. 4: Variation of ultimate load, P_u obtained from FEA and using DSM expressions with respect to non-dimensional slenderness ratio, λ for specimens with thickness (a) t = 1.2 mm and (b) t = 2 mm respectively

4. Results and discussions

The Table. 2 reports dimension details, material properties, ultimate web crippling load from FEA ($P_{u\text{-}FEA}$). Furthermore, the accuracy of the DSM expression proposed by [15] is also checked against the FE model results by calculating ($P_{u\text{-}DSM}$ / $P_{u\text{-}FEA}$) values and reported in same table. The variation of ultimate load obtained from FEA, $P_{u\text{-}}$ using DSM expressions, $P_{u\text{-}DSM}$ with respect to non-dimensional slenderness ratio, λ for specimens with thickness (a) t = 1.2 mm and (b) t = 2 mm respectively (Fig. 4). Here, the yield load, P_y is calculated using Eqn. 2b as given in [15]. The results obtained from the DSM approach yielded conservative estimates, as indicated by the ratio of ($P_{u\text{-}DSM}$ / $P_{u\text{-}FEA}$) being less than 1, as reported in Table. 2. These results underestimated the web crippling capacity obtained from the FE model for most specimens, except for those with small λ values and specific section thickness (t = 1.2 mm) and width of bearing plate (N = 150 mm), as shown in Fig. 4(a). The mean (μ) and COV of the ($P_{u\text{-}DSM}$ / $P_{u\text{-}FEA}$) ratio is 0.879 and 0.112 respectively. Additionally, it is important to acknowledge that when considering DSM based results, there is a more significant decrease in strength as the value of λ increases, especially for larger values of N, in comparison to the FEA results. The parametric study thus yielded valuable insights into the web crippling behavior of LCB sections, which showed that the web slenderness ratio (h/t and P_{cr}) has negligible effect on web crippling strength. These finding suggests that web crippling may not solely be attributed to buckling, which challenges the suitability of DSM based methods for addressing this phenomenon. Hence, these observations raise concerns regarding the appropriateness of employing a DSM-based methodology for designing CFS sections to resist web crippling.

Table 2: Dimension details, elastic buckling strength and ultimate web crippling loads obtained from FEA and predicted using DSM expression for parametric study.

Name	H	B	h/t	N = 50 mm				N = 100 mm				N = 150 mm			
	(mm)	(mm)		P_{cr} (kN)	λ	P_{u-FEA} (kN)	$\frac{P_{u-DSM}}{P_{u-FEA}}$	P_{cr} (kN)	λ	P_{u-FEA} (kN)	$\frac{P_{u-DSM}}{P_{u-FEA}}$	P_{cr} (kN)	λ	P_{u-FEA} (kN)	$\frac{P_{u-DSM}}{P_{u-FEA}}$
100-t1.2	100	40	74.7	14.65	0.61	7.931	0.843	18.78	0.62	8.978	0.984	23.54	0.68	9.893	1.277
150-t1.2	150	50	116	8.936	0.9	7.768	0.873	10.53	0.94	8.945	0.937	12.29	0.94	9.226	1.068
200-t1.2	200	60	158	6.412	1.18	7.447	0.859	7.248	1.23	8.52	0.886	8.142	1.27	8.743	0.997
250-t1.2	250	80	200	4.979	1.46	7.52	0.809	5.5	1.52	8.539	0.817	6.045	1.56	8.651	0.91
300-t1.2	300	120	241	4.034	1.74	7.242	0.802	4.401	1.81	8.626	0.758	4.766	1.86	8.857	0.82
350-t1.2	350	130	283	3.416	2.02	6.925	0.81	3.672	2.09	7.897	0.787	3.955	2.14	7.962	0.858
150-t2	150	50	69	41.45	0.58	21.082	0.836	48.93	0.61	26.242	0.849	57.73	0.61	28.497	0.925
200-t2	200	60	94	29.66	0.77	20.742	0.904	33.59	0.74	25.862	0.868	38.05	0.82	27.317	0.961
250-t2	250	80	119	22.98	0.95	20.56	0.904	25.41	0.99	25.813	0.829	28.11	1.02	26.806	0.906
300-t2	300	120	144	18.63	1.14	20.66	0.872	20.3	1.18	26.386	0.771	22.14	1.21	27.432	0.828
350-t2	350	130	169	15.77	1.32	20.427	0.861	16.97	1.37	25.534	0.764	18.27	1.4	26.2	0.821

5. Conclusion

The present study provides a comprehensive analysis of the validation and numerical investigation of cold-formed LCBs that are fastened with flanges. The study focusses specifically on the behaviour of these sections under ITF loading. This study constructs FE models utilising ABAQUS/CAE 2020 that models web crippling phenomenon accurately, conduct linear perturbation analysis to calculate the critical buckling load (P_{cr}) and perform a non-linear static analysis to determine the ultimate load (P_u). The paper provides a comprehensive explanation of the procedure followed in the modelling process. The parametric study revealed the web crippling behaviour of LCB sections

showing the minimal impact of web slenderness ratio (expressed using h/t and P_{cr}) on the web crippling capacity. The revelation that web crippling is primarily caused by factors other than buckling challenges the validity of DSM-based approaches to understanding this phenomenon. These results raise questions about the appropriateness of using DSM-based based CFS section design for web crippling and emphasise the importance of conducting more comprehensive studies for a for a better understanding of the web crippling behaviour of LCBs sections.

References

[1] EN 1993-1-3, *Eurocode 3: Design of steel structures-Part 1-1: General rules and rules for buildings*. 2006.

[2] American Institute of Steel Construction, *North American Specification for the Design of Cold-Formed Steel Structural Members, 2016 Edition (Reaffirmed 2020) With Supplement 2, 2020 Edition*. American Institute of Steel Construction, Incorporated, 2016.

[3] American Institute of Steel Construction S909, "Standard test method for determining the web crippling strength of cold-formed steel beams," 2013, *AISI Washington, DC*.

[4] K. S. Sivakumaran, "Analysis for web crippling behaviour of cold-formed steel members," *Comput Struct*, vol. 32, no. 3–4, pp. 707–719, 1989.

[5] M. Macdonald, M. A. H. Don, M. KoteŁko, and J. Rhodes, "Web crippling behaviour of thin-walled lipped channel beams," *Thin-Walled Structures*, vol. 49, no. 5, pp. 682–690, 2011.

[6] M. Macdonald and M. A. Heiyantuduwa, "A design rule for web crippling of cold-formed steel lipped channel beams based on nonlinear FEA," *Thin-Walled Structures*, vol. 53, pp. 123–130, 2012.

[7] A. Uzzaman, J. B. P. Lim, D. Nash, J. Rhodes, and B. Young, "Web crippling behaviour of cold-formed steel channel sections with offset web holes subjected to interior-two-flange loading," *Thin-Walled Structures*, vol. 50, no. 1, pp. 76–86, 2012.

[8] Y. Chen, X. Chen, and C. Wang, "Experimental and finite element analysis research on cold-formed steel lipped channel beams under web crippling," *Thin-Walled Structures*, vol. 87, pp. 41–52, 2015, doi: 10.1016/j.tws.2014.10.017.

[9] R. A. J. Heurkens, H. Hofmeyer, M. Mahendran, and H. H. Snijder, "Direct strength method for web crippling—Lipped channels under EOF and IOF loading," *Thin-Walled Structures*, vol. 123, pp. 126–141, Feb. 2018, doi: 10.1016/j.tws.2017.11.008.

[10] P. Natário, N. Silvestre, and D. Camotim, "Web crippling failure using quasi-static FE models," *Thin-Walled Structures*, vol. 84, pp. 34–49, 2014.

[11] P. Natário, N. Silvestre, and D. Camotim, "Web crippling of beams under ITF loading: A novel DSM-based design approach," *J Constr Steel Res*, vol. 128, pp. 812–824, 2017.

[12] L. Sundararajah, M. Mahendran, and P. Keerthan, "New design rules for lipped channel beams subject to web crippling under two-flange load cases," *Thin-Walled Structures*, vol. 119, pp. 421–437, 2017.

[13] B. W. Schafer and T. Peköz, "Direct strength prediction of cold-formed steel members using numerical elastic buckling solutions," in *Fourteenth International Specialty Conference on Cold-Formed Steel Structures St. Louis, Missouri*, 1998.

[14] M. Y. Choy, X. F. Jia, X. Yuan, J. Zhou, H. S. Wang, and C. Yu, "Direct strength method for web crippling of cold-formed steel C-and Z-sections subjected to two-flange loading," in *Proceedings of the annual stability conference structural stability research council*, 2014, pp. 99–111.

[15] V. V. Nguyen, G. J. Hancock, and C. H. Pham, "Consistent and Simplified Direct Strength Method for Design of Cold-Formed Steel Structural Members under Localized Loading," *Journal of Structural Engineering*, vol. 146, no. 6, p. 4020090, 2020.

[16] S. Gunalan and M. Mahendran, "Web crippling tests of cold-formed steel channels under two flange load cases," *J Constr Steel Res*, vol. 110, pp. 1–15, 2015, doi: 10.1016/j.jcsr.2015.01.018.

[17] L. Sundararajah, M. Mahendran, and P. Keerthan, "New web crippling design rules for cold-formed steel beams," 2018.

[18] Y. Lian, A. Uzzaman, J. B. P. Lim, G. Abdelal, D. Nash, and B. Young, "Effect of web holes on web crippling strength of cold-formed steel channel sections under end-one-flange loading condition–Part I: Tests and finite element analysis," *Thin-Walled Structures*, vol. 107, pp. 443–452, 2016.

[19] Y. Lian, A. Uzzaman, J. B. P. Lim, G. Abdelal, D. Nash, and B. Young, "Web crippling behaviour of cold-formed steel channel sections with web holes subjected to interior-one-flange loading condition–Part II: parametric study and proposed design equations," *Thin-Walled Structures*, vol. 114, pp. 92–106, 2017.

[20] B. Beshara and R. M. Schuster, "Web Crippling of Cold Formed Steel C-and Z- Sections," 2000. [Online]. Available: https://scholarsmine.mst.edu/isccss/15iccfss/15iccfss-session2/6

[21] K. Prabakaran and R. M. Schuster, "Web Crippling of Cold Formed Steel Members," 1998. [Online]. Available: https://scholarsmine.mst.edu/isccss/14iccfsss/14iccfsss-session3/2

[22] L. Sundararajah, M. Mahendran, and P. Keerthan, "Numerical modeling and design of lipped channel beams subject to web crippling under one-flange load cases," *Journal of Structural Engineering*, vol. 145, no. 10, p. 4019094, 2019.